Downloaded from rsta.royalsocietypublishing.org

PHILOSOPHICAL TRANSACTIONS OF THE ROYAL SOCIETY A MATHEMATICAL, PHYSICAL & ENGINEERING SCIENCES

Mobile Tracers: Their Use in Understanding Key Features of Anodic Alumina Film Formation

P. Skeldon, K. Shimizu, G. E. Thompson and G. C. Wood

Phil. Trans. R. Soc. Lond. A 1994 **348**, 295-314
doi: 10.1098/rsta.1994.0092

Email alerting service

Receive free email alerts when new articles cite this article - sign up in the box at the top right-hand corner of the article or click **here**

To subscribe to *Phil. Trans. R. Soc. Lond. A* go to:
http://rsta.royalsocietypublishing.org/subscriptions

This journal is © 1994 The Royal Society

Downloaded from rsta.royalsocietypublishing.org

Mobile tracers: their use in understanding key features of anodic alumina film formation

By P. Skeldon[1], K. Shimizu[2], G. E. Thompson[1] and G. C. Wood[1]

[1] *Corrosion and Protection Centre, University of Manchester, Institute of Science and Technology, P.O. Box 88, Manchester M60 1QD, U.K.*

[2] *Department of Chemistry, Faculty of Science and Technology, Keio University, 3-14-1 Hiyoshi, Yokohama 223, Japan*

A novel procedure is described for incorporating layers of alumina, contaminated with species derived from the electrolyte, e.g. molybdenum species, within anodic films, for application in the study of mobility and growth mechanisms of anodic barrier films on aluminium. Use of these mobile tracers shows that anodic alumina, developed at a high current efficiency, forms at the metal/film and film/electrolyte interfaces with no significant formation within the film bulk. The outward mobility of incorporated molybdenum species, the tracer, was found to be unchanged throughout the film regions. Indeed, the movements of the various species during anodizing are fully accounted for by use of their usual transport numbers. Occasional anomalous behaviour is observed locally during film growth at and in the vicinity of flaws, probably owing to local current concentration at the flaw site, and when chromium-containing layers are used as tracers. In the latter situation, voids and cracks are revealed in the contaminated alumina, possibly arising from the development of a crystalline alumina containing incorporated chromium species.

1. Introduction

The growth mechanisms of barrier-type anodic films on valve metals, particularly aluminium and tantalum, have been a source of fascination to investigators for many years, stimulating numerous studies. The importance of these studies reflects the crucial roles that films frequently play in controlling metal passivity and the various forms of corrosion and degradation. Furthermore, the barrier films considered here may well prove to be thicker versions of the passive films encountered more generally, as well as having widespread use in electronics. Although earlier experimental and theoretical work established a broad understanding of film formation, primarily based on the high-field conduction model (Young 1961), many important aspects were obscure. Indeed, only with the advent of radioactive tracers (Davies *et al.* 1965), ion implantation (Brown & Mackintosh 1973) and nuclear analytical techniques (Amsel & Samuel 1962) has ionic transport through the films been investigated directly, revealing both cation and anion fluxes, with migration proceeding via an unresolved complex process, suggested to involve cations and anions in a cooperative manner (Amsel & Samuel 1962). Later, further progress was made when films formed on aluminium were sectioned by ultramicrotomy (Furneaux *et al.* 1978), enabling direct observation in the transmission electron microscope (TEM) with analytical facilities (energy-dispersive X-ray analysis (EDX) and electron energy loss spectroscopy (EELS)) of transport phenomena, such as the consistent but

Phil. Trans. R. Soc. Lond. A (1994) **348**, 295–314
Printed in Great Britain

© 1994 The Royal Society

The Royal Society is collaborating with JSTOR to digitize, preserve, and extend access to *Philosophical Transactions: Physical Sciences and Engineering.* www.jstor.org

Downloaded from rsta.royalsocietypublishing.org

diverse distribution and mobility of incorporated species characteristic of the electrolyte (Shimizu *et al.* 1981).

Of practical importance, several species containing elements of high atomic number were readily visible in electron micrographs of sections, because the regions of the film in which they were confined appeared darker, owing to the increased electron scattering caused by their presence, with the boundary between the contaminated (i.e. containing the incorporated species) and pure alumina being relatively sharp (Skeldon *et al.* 1985). These species are mobile, moving outwards as a result of a field-induced transformation of the originally adsorbed or incorporated anions but at a lower rate than aluminium species, and appeared as a darker band in film regions extending inwards from the film/electrolyte interface. The relative ease of observation, coupled with the high spatial resolution of the TEM, suggests the application of these contaminated layers as mobile tracers which could be used to study ionic mobility, electric field uniformity, space charge effects, film formation sites, film growth conditions surrounding flaws, etc. This paper describes the method for positioning such contaminated layers precisely within films, i.e. displaced from their usual positions adjacent to the film/electrolyte interface, so that their subsequent migration and behaviour within the film during anodizing may be observed. Specifically, studies have been made of the incorporation of electrolyte species, mobile and immobile, with quantification of the outward movement of mobile tracers. Additionally, the proportions of film developing at the metal/film and film/electrolyte interfaces have been determined using inert and immobile argon markers. Finally, limited assessment of the film growth behaviour in the vicinity of flaws, always present in films on aluminium, has been made.

The procedure used may prove to be of wide application and value because repositioning of contaminated layers, mobile or immobile, may be beneficial to studies of breakdown, rectification, construction of electronic devices, etc. As mobile tracers, such contaminated layers are in some ways more realistic than ion-implanted species or marker layers, whose implantation may cause structural damage and locate ions in atypical sites or create bubbles, etc., whereas the contaminated layers are naturally an integral part of the anodic film.

2. Experimental

(*a*) *Sample preparation*

Foils of superpure aluminium (0.003 %Fe; 0.004 %Cu; 0.002 % (by mass) Si), of dimensions 30 mm × 10 mm × 0.1 mm, were electropolished at 20 V in stirred 75 % perchloric acid/ethanol (20/80 by volume) at 273–278 K for 2 min. After electropolishing, the foils were carefully washed with double-distilled water and Analar grade acetone before drying in a cool air stream. About 10 mm of one end of each foil was then insulated by forming a relatively thick anodic film at approximately 100 A m^{-2} in dilute ammonium pentaborate electrolyte to about 600 V at room temperature (*ca.* 293 K), ensuring that the remaining electropolished areas were kept uncontaminated; the sample was then thoroughly washed and dried. A drop of insulating lacquer (Lacomit) was placed approximately in the centre of one electropolished face of each sample and given about 20 h to dry at room temperature. The dried lacquer formed a disc of about 6 mm diameter (figure 1*a*; the initial anodic film, formed to 600 V, is not shown in the figure). The samples were then anodized to selected voltages (typically 75 V) at a constant current density of 50 A m^{-2} in the

PHILOSOPHICAL TRANSACTIONS OF THE ROYAL SOCIETY A MATHEMATICAL, PHYSICAL & ENGINEERING SCIENCES
PHILOSOPHICAL TRANSACTIONS OF THE ROYAL SOCIETY A MATHEMATICAL, PHYSICAL & ENGINEERING SCIENCES

Downloaded from rsta.royalsocietypublishing.org

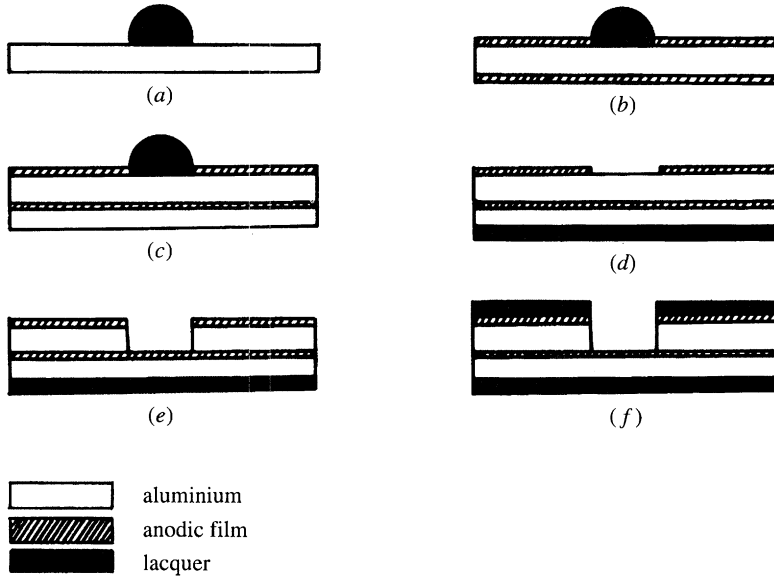

Figure 1. Schematic diagram of the procedure adopted for specimen preparation: (*a*) Electropolished aluminium with a drop of Lacomit on one of the exposed faces. (*b*) Anodizing after (*a*) develops a barrier-type anodic film on the exposed faces. (*c*) Ion plating of an aluminium layer above the original anodic film on the opposite side from the Lacomit. (*d*) Removal of the original drop and masking of the ion plated layer. (*e*) Electropolishing of (*d*) to remove the exposed part of the original aluminium substrate. (*f*) After further masking, the final specimen is ready for anodizing of the ion plated aluminium beneath the originally formed anodic film. Note that the ion plated aluminium is present at the original film/electrolyte interface.

chosen electrolyte (ammonium pentaborate, sodium chromate, sodium molybdate or sodium tungstate) under conditions in which films form at 100% efficiency and at about 1.18 nm V^{-1} at 293 K (figure 1*b*). Electrolytes were prepared from Analar grade reagents and double-distilled water and were continuously stirred throughout anodizing. The accuracy with which the anodizing voltage was measured was ± 2 V. Samples were washed and dried as usual, then stored in a desiccator until the next stage of preparation.

Subsequently, samples were placed in an ion-plating unit with the non-spot lacquered side exposed for coating. A brief argon ion etch was then given to remove contaminants from the film surfaces, immediately followed by ion plating with a relatively thick (*ca.* 5 μm) layer of aluminium (figure 1*c*). The samples were removed from the unit and, after stripping of the lacquer, prepared for a second anodizing stage by immersing each sample in Analar grade acetone, followed by subsequent rinses in fresh Analar grade acetone and drying in a cool air-stream. Lacquer was then re-applied to the sample, although on the reverse face to the original application, ensuring that the aluminium plated face was fully covered. Again the lacquer was given about 20 h to cure (figure 1*d*).

Next, the samples were electropolished at 20 V in the usual mixture at 273 K until the current diminished to a low value, which typically took about 90 min. At this stage, all of the aluminium under the original lacquer spot was removed (figure 1*e*). It should be noted that during this period of electropolishing it was essential that the polishing solution was unstirred and that the sample was held vertically, so that the natural convection established caused the most rapid polishing at the top of the

Downloaded from rsta.royalsocietypublishing.org

exposed region of aluminium; the downward flow of viscous polishing products presumably hindered polishing at lower levels. Otherwise, if stirring was used, residual islands of aluminium remained attached to the insulating anodic alumina at the base of the polished area, probably because of slight non-uniformity in the aluminium thickness. During the electropolishing process, the bath temperature was monitored closely to ensure there were no significant temperature rises in the highly oxidizing electrolyte. It has already been established that this type of polishing procedure causes no significant damage to exposed anodic alumina films (Shimizu *et al.* 1982). Furthermore, the lacquer is resistant to the polishing solution, and shields covered areas from attack.

Successful completion of polishing resulted in an unlacquered face covered by anodic film on the original aluminium substrate, except at the area of the initial lacquer spot which prevented anodizing; at this area the aluminium substrate had now been completely polished away to reveal the anodic film on the opposite face of the sample, which was now on a substrate of ion-plated aluminium supported by lacquer. This region, being thin, was delicate and samples required gentle handling. Final rinsing was performed in double-distilled water with cool air-drying. The newly exposed film now contained the anion contaminated part of the anodic film at its metal/film interface.

Next, lacquer was applied to the presently unlacquered face except at the region from which the original aluminium substrate had been removed by electropolishing, giving a sample completely lacquered except for the insulated end and this latter region (figure 1*f*). After drying, the samples were anodized under the previous conditions to various voltages, including some to the breakdown voltages in the chosen electrolyte. The fresh film material was formed though the exposed region at which the original film was attached to the ion-plated aluminium substrate, i.e. the region at which the original metal/film interface and film/electrolyte interface had been reversed by the previous procedure. Anodized samples were washed in double-distilled water and Analar grade acetone and dried in a cool air-stream.

(*b*) *Examination and analysis*

Sections of the films were cut on an LKB III ultramicrotome, by the previously published procedure (Furneaux *et al.* 1978) and examined, in the bright-field mode, in a Philips 301 transmission electron microscope. The morphology of ion-plated layers was studied in a Hitachi S450 scanning electron microscope. The compositions of films formed on selected anodized samples were determined by Rutherford backscattering spectroscopy (RBS) using elastic scattering of 2 MeV α-particles in the 7 MeV Van de Graaff accelerator at the University of Manchester; details of the experimental arrangement have been given elsewhere (Skeldon *et al.* 1983).

3. Results and discussion

Important features of barrier film growth over the macroscopic aluminium surface are considered in the following sections together with limited information on local or flaw behaviour. In making use of tracer layers or other contaminated film regions, some variation in anodizing conditions has been used to allow an experimental procedure which gives the most reliable and sensitive results. An important feature in describing film growth is the use of appropriate reference planes, e.g. metal/film or film/electrolyte interfaces, as well as the location of any marker or tracer regions.

PHILOSOPHICAL TRANSACTIONS OF THE ROYAL SOCIETY A MATHEMATICAL, PHYSICAL & ENGINEERING SCIENCES

PHILOSOPHICAL TRANSACTIONS OF THE ROYAL SOCIETY A MATHEMATICAL, PHYSICAL & ENGINEERING SCIENCES

Downloaded from rsta.royalsocietypublishing.org

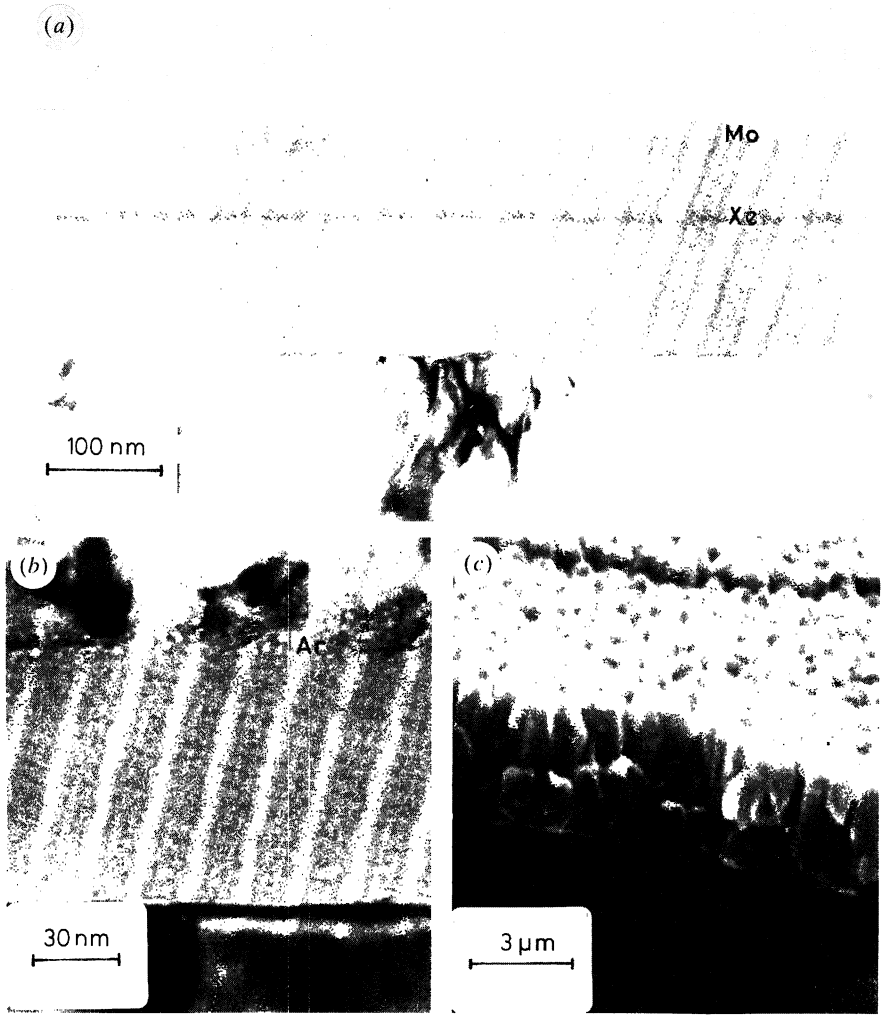

Figure 2. Electron micrographs of variously developed anodic alumina films on aluminium substrates. (*a*) Transmission electron micrograph of an ultramicrotomed section of the film formed on electropolished aluminium to 175 V at 50 A m^{-2} in 0.1 M sodium molybdate electrolyte at 293 K. (*b*) Transmission electron micrograph of the ultramicrotomed section of the original anodic film, formed to 75 V at 50 A m^{-2} in 0.1 M sodium molybdate electrolyte at 293 K, sandwiched between the ion plated aluminium and original electropolished aluminium substrate. (*c*) Scanning electron micrograph of the fracture section of the ion plated aluminium, showing the columnar grain appearance.

In view of the finite widths of many of these regions, care must be exercised in the selection of the correct location from which measurements are made. Thus, the case for reference to locations just above argon bubbles is made in the Appendix.

(*a*) *Morphology and composition of individual films formed in molybdate electrolyte*

A transmission electron micrograph of an ultramicrotomed section of the anodic film formed on electropolished aluminium in molybdate electrolyte is revealed in figure 2*a*, with the typical atomic number contrast effect, arising from incorporated molybdenum, evident in the outer film regions. The film was formed from a thin pre-

Downloaded from rsta.royalsocietypublishing.org

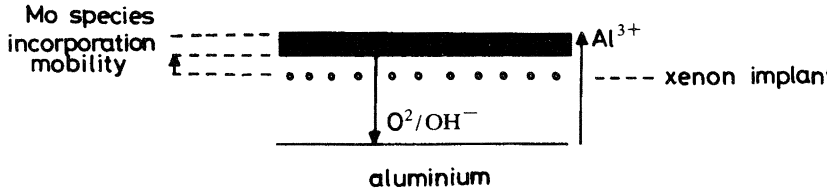

Figure 3. Schematic diagram showing the locations of various regions within the anodic film, formed to 175 V at 50 A m^{-2} in 0.1 M sodium molybdate electrolyte at 293 K.

existing anodic film containing an ion-implanted layer of xenon which is immobile during film growth. Such films have been characterized previously by both direct observation in the TEM and RBS and are known to consist principally of pure anodic alumina except for an outermost film region, representing about 0.2 of the total film thickness, which contains molybdenum incorporated from the electrolyte during film growth. The molybdenum is uniformly distributed in the contaminated layer, which is of constant thickness across the section (Skeldon *et al.* 1989); the total amount of molybdenum in the film is only about 0.24 at. %.

The schematic diagram of figure 3 shows the location of the various film regions with reference to an inert xenon marker layer, originally within a thin pre-formed film. On the recognized premise that the anodic alumina above the marker layer develops by Al^{3+} egress through the pre-existing film and that below the marker layer is formed though O^{2-} and/or OH^- ingress (Hoar & Mott 1959), an apparent cation transport number of 0.4 can be defined. Importantly, the molybdenum-containing film region is located within the outer film regions but significantly distanced from the marker layer. This appearance indicates the presence of an outwardly mobile molybdenum species; immobile species would be resident throughout the outer film region and inwardly mobile species would migrate into the inner pure alumina film region. To explain this behaviour it is envisaged that molybdate ions are initially adsorbed at the film/electrolyte interface and incorporated into the developing alumina. After absorption or incorporation, the oxy-anion is apparently transformed under the field, with the resultant species being outwardly mobile; for outward mobility it is evident that the migrating species is positively charged, with a mobility under the field less than that of Al^{3+} egress, i.e. approximately one half of that of aluminium species. Thus, O^{2-} ions have been stripped from the molybdate anion yielding a species such as MoO_2^{2+}; further stripping of oxygen may eventually generate Mo^{6+} as the outwardly mobile species.

(*b*) *Film morphology after substrate reversal*

Before individual diagnostic experiments with the films after substrate reversal, the film section was observed immediately after ion plating of aluminium onto the original film/electrolyte interface. Thus, the transmission electron micrograph of the ultramicrotomed section of figure 2*b* reveals the film sandwiched between the original substrate (lower region) and the plated substrate (upper region). Along the ion-plated metal/film interface, just within the anodic film, a linear region of fine bubbles is evident. Such bubbles represent retained argon, arising from limited ion cleaning of the film surface before plating of aluminium; the bubbles are not the result of interface porosity due to poor substrate bonding. Furthermore, the micrograph reveals that the ion-plating conditions have not caused significant damage to the original film surface which would have obliterated the 'bubble-

Downloaded from rsta.royalsocietypublishing.org

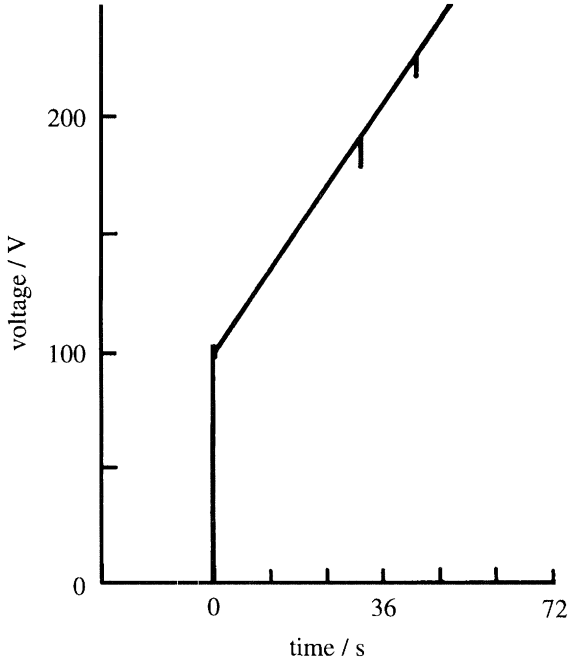

Figure 4. Typical voltage–time behaviour in the second anodizing stage, for a specimen bearing a film formed to 100 V in the first anodizing treatment. Occasional voltage spikes are evident, reflecting breakdown of the insulating lacquer, but not interfering significantly with the main film regrowth process.

containing' layer, although there may be limited aluminium penetration into finely porous regions of the film at the outermost surface. Further confirmation of the lack of damage or degradation of the film as a consequence of argon ion etching/aluminium plating is given from comparison of the original film thickness with that of the film in the sandwich of figure 2*b*. The film thickness, measured from the micrograph, is 86.3 ± 2.6 nm which agrees closely with the anticipated film thickness through anodizing in molybdate electrolyte to 75 V, i.e. 88.5 nm.

Generally, for success in the application of relatively thin aluminium layers to anodic alumina, the plating conditions must be selected to give good adhesion but avoiding either significant penetration of aluminium into the exposed film regions (which is obviously undesirable in that the metal/film interface cannot be precisely defined) or poor bonding which results in delamination and buckling during subsequent film growth.

A scanning electron micrograph of the fracture section of a successfully plated aluminium layer is shown in figure 2*c*; the general columnar texture of the *ca.* 5 μm thick coating is revealed and is of grain size about 1 μm, with no porosity evident.

(*c*) *General re-anodizing behaviour after substrate reversal*

A voltage–time curve for a typical sample is shown in figure 4; the voltage initially rises immediately to a value equal within experimental accuracy (2 V) to the terminating anodizing voltage of the initially formed film (stage 1 film), indicating that electropolishing had not caused significant thinning or opening of flaws, pinholes, etc. The voltage then increased smoothly and linearly as new film was added.

Downloaded from rsta.royalsocietypublishing.org

The constancy of the slope further indicated that the film/substrate interface was uniform and free of pores or other artefacts which would hinder anodizing, the samples behaving as would be expected if normal film growth had merely been halted and restarted. Spikes appeared intermittently on traces as the voltage suddenly decreased and then resumed its value. These were almost certainly caused by occasional local failures at lacquered regions. These breakdown regions did not reveal sufficient areas to decrease current densities at regions of interest, as could be seen from the insignificant changes in the slope of the voltage–time curves. Occasionally, samples suffered excessive breakdown, particularly at high voltages, but these were rejected from analysis. Considering that all the samples discussed in this paper were obtained at the first attempt, it may be concluded that the approach is successful and greater experience would probably eliminate almost entirely the relatively few rejections.

(*d*) *Locations of film growth and mobility of incorporated molybdenum: duplex films formed in molybdate and borate electrolytes*

The advantages to be gained from re-anodizing of films after substrate reversal, developing duplex films, can be easily clarified by considering a specific example. Here, a film was formed by a first stage anodizing in 0.1 M molybdate electrolyte to 75 V and a second stage anodizing in 0.01 M borate electrolyte to 295 V (i.e. total anodizing voltage); the individual procedures are indicated in the schematic diagram of figure 5 and the ultramicrotomed section of the resultant film is shown in figure 6*a*. The usual anodic film characteristics, comprising relatively flat metal/film and film/electrolyte interfaces, and uniformly textured, generally featureless anodic alumina are observed. However, in addition, two bands of differing contrast and texture, running parallel to the previous interfaces are visible and are seen more clearly in the high magnification micrograph of the film section (figure 6*b*). Other bands of varying contrast running at a slight angle to the interfaces are marks from the diamond knife used to cut the sections; such marks change direction with variation in cutting direction, whereas the location of the previously mentioned bands remain unchanged. The outer band that is closer to the film/electrolyte interface is of the same featureless appearance as the majority of the film, but of darker shade. This contrast results from incorporation of an element into the film of higher atomic number than the adjacent regions, which causes greater electron scattering and thus gives a darker appearance. The element is molybdenum, incorporated during the first stage of anodizing. The inner band, nearer to the metal/film interface, is of slightly lighter shade, and upon close inspection is seen to consist of fine bubbles, less than or of the order of 3 nm diameter, which resulted from implantation of argon during etching of the film to clean the surface prior to plating of aluminium. Similar bubbles are observed in ultramicrotomed sections of films deliberately implanted with inert gases as a separate procedure (Shimizu *et al.* 1982*a*).

Because it has already been established that implanted inert gas marker layers of xenon, of similar appearance to the argon etch inner band, are immobile during film growth and do not significantly affect ionic transport (Pringle 1973; Shimizu *et al.* 1982*a*), it can be reasonably assumed that the argon etch band represents an inert, immobile marker layer to which ionic migration and film growth can be referred. Thus, the argon etch band marks the position of the metal/film interface at the start of the second stage anodizing. Hence, new film formed in this stage at the metal/film

Downloaded from rsta.royalsocietypublishing.org

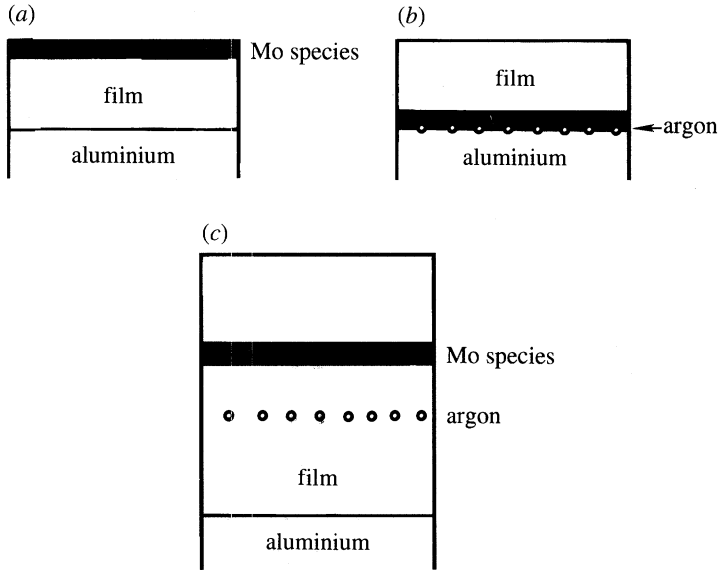

Figure 5. Schematic diagrams of the appearance of the anodic film in section after various forming operations. (*a*) Film growth to 75 V at 50 A m^{-2} in 0.1 M sodium molybdate electrolyte at 293 K. (*b*) After substrate reversal. (*c*) After substrate reversal and re-anodizing to 295 V at 50 A m^{-2} in 0.01 M ammonium pentaborate electrolyte.

interface must form below this layer, i.e. the portion of film between the argon etch band and the metal/film interface represents that part of the film formed during the second stage of anodizing by inward migration of O^{2-}/OH^{-} ions, assuming reaction occurs only at the interfaces and not within the film, which is generally accepted. Conversely and obviously, the part formed at the film/electrolyte interface by outward migration of aluminium ions resides above this band.

Inspection of figures 5 and 6 shows that the incorporated molybdenum is undoubtedly mobile, moving towards the film/electrolyte interface; the region of film between the molybdenum-contaminated layer and the argon etch band is now evidently molybdenum-free because no contrast in shade with the pure film material is present. Thus, the sample preparation procedure has enabled the molybdenum-contaminated layer to move through a region of pure alumina film in which it does not normally exist because, under usual anodizing conditions, this layer is always located at the film surface. Additionally, in the duplex film, the molybdenum species has maintained its usual behaviour of outward mobility.

(*e*) *Development of material within the anodic film: duplex films formed in borate electrolytes*

To quantify the migration of incorporated molybdenum species it is first necessary to ensure that the sample preparation has caused no subtle anomalies in film growth such as a changed nanometre per volt ratio for the second stage of anodizing. This is readily eliminated by reference to figure 6 where total film thicknesses, after second stage anodizing, measured in the TEM, were equal to the calculated values using the final voltage and the usual formation ratio of 1.18 nm V^{-1}, to an accuracy of about 3%. Hence, during the second stage of anodizing, film growth occurs at the same rate as during the first stage. Thus, there is a constant relation between voltage and film

Downloaded from rsta.royalsocietypublishing.org

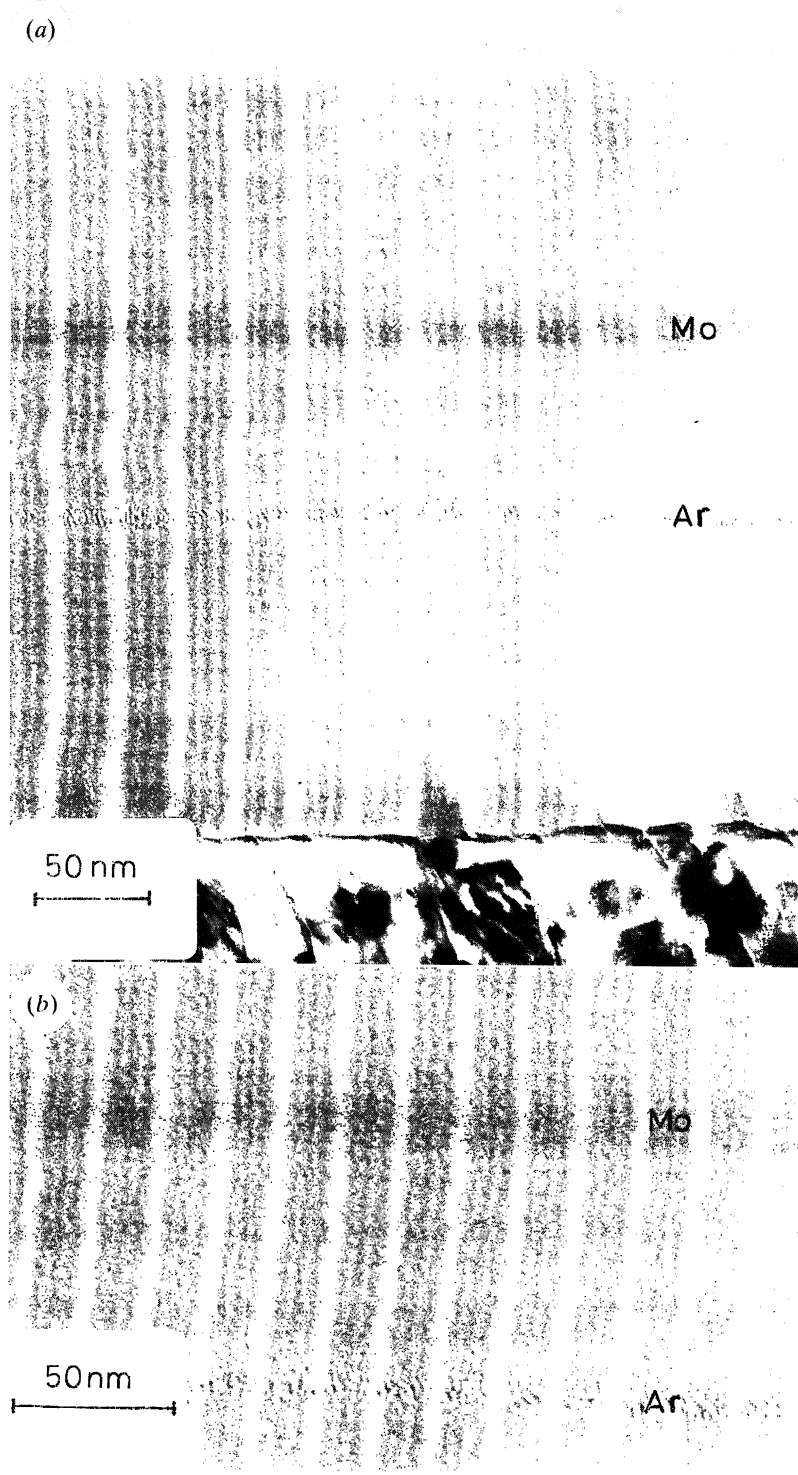

Figure 6. For description see opposite.

PHILOSOPHICAL TRANSACTIONS OF THE ROYAL SOCIETY A MATHEMATICAL, PHYSICAL & ENGINEERING SCIENCES
PHILOSOPHICAL TRANSACTIONS OF THE ROYAL SOCIETY A MATHEMATICAL, PHYSICAL & ENGINEERING SCIENCES

Downloaded from rsta.royalsocietypublishing.org

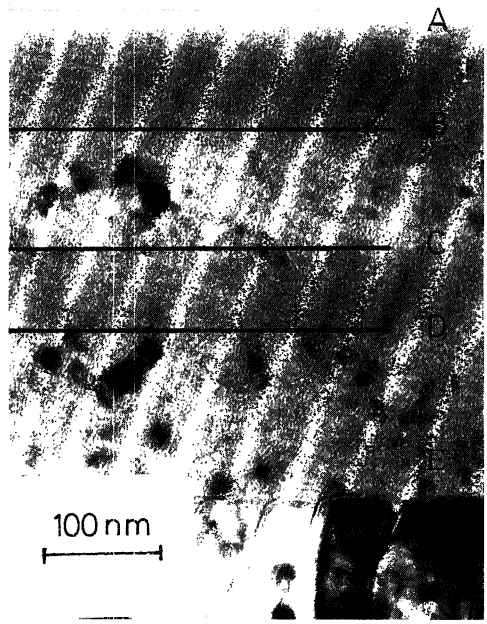

Figure 7. Transmission electron micrograph of an ultramicrotomed section of the anodic film attached to the ion plated aluminium substrate. The first anodizing stage involved film formation to 150 V at 50 A m^{-2} in 0.1 M ammonium pentaborate borate electrolyte at 293 K; the second stage involved re-anodizing to 355 V under the same conditions. Electron beam induced crystallization distinguishes the various film regions present: *AB* and *CD* are contaminated with boron species, whereas *BC* and *DE* are crystallized regions of relatively pure alumina.

thickness throughout the whole anodizing procedure, such that the interface reversal of the first stage film has not introduced any anisotropy. Migration must also be separated from apparent movements which could be caused by swelling of the film bulk that would occur if it was necessary to accommodate new film material formed by reactions of the ionic fluxes within the film. This may be examined by observing dimensional changes in a contaminated layer (from the first stage of anodizing) during the second stage of anodizing, because new film formed within the original contaminated layer would result in an increase in its thickness. The study was made with a film formed in 0.1 M ammonium pentaborate electrolyte in both stages because the contaminated layer of the first stage represents about 0.4 of the first stage thickness (Shimizu *et al.* 1982*b*), thus being of greater width than the

Figure 6. Transmission electron micrograph of an ultramicrotomed section of the anodic film attached to the ion plated aluminium substrate. The first anodizing stage involved film formation to 75 V at 50 A m^{-2} in 0.1 M sodium molybdate electrolyte at 293 K; the second stage involved re-anodizing to 295 V at 50 A m^{-2} in 0.01 M ammonium pentaborate electrolyte at 50 A m^{-2}. (*a*) Typical appearance of the film section with the molybdenum species containing region (Mo) and argon bubbles (Ar) indicated. (*b*) Higher magnification micrograph of (*a*), showing the argon bubbles and the molybdenum-containing film region.

Downloaded from rsta.royalsocietypublishing.org

molybdenum-contaminated layer for equal first voltages, enabling easier measurement. The film was partly crystallized in the TEM in the usual way (Shimizu *et al.* 1982*b*) to reveal the uncrystallized contaminated layers containing boron. Figure 7 shows the partly crystallized film formed by anodizing to 150 V in the first stage and re-anodizing to a final voltage of 355 V; the interfaces between various film regions have been delineated for clarity. The contaminated layers are free of crystalline alumina; boron, of lower atomic number than aluminium and oxygen, does not assist observation of the contaminated film regions, unlike molybdenum, and so the crystallization procedure is essential to reveal its region of incorporation in the alumina film material. Boron is well established as an immobile species when incorporated into a film formed in an aqueous electrolyte, being distributed uniformly throughout the outer 0.4 of the film (Shimizu *et al.* 1982*b*). Thus, the interface at D in figure 7 corresponds to the position of the original ion-plated/first stage anodic film interface, i.e. the location of the argon etch band, which is not evident in the micrograph in the focus condition used. ED represents the new relatively pure alumina laid down during the second anodizing stage. The outer band between A and B is new material added at the film surface during the second stage of anodizing, because boron, being immobile, is distributed throughout this fresh film. Thus, the region between B and D must correspond to the first stage film through which the ionic fluxes have passed to form the interfacial layers AB and DE during the second stage. The ratio of the sum of the thicknesses of AB and DE to the total film thickness is 0.60 ± 0.02, which compares well with the expected ratio of the second stage voltage to the total voltage of 0.58 ± 0.01; hence, film material must be created at the interfaces and not within the film. Furthermore, the relative thicknesses of the boron-contaminated layers for the first and second stages of anodizing are 0.37 ± 0.03 and 0.41 ± 0.02, in good agreement with the result normally found for a crystallized film formed in a single anodizing stage (*ca.* 0.4). Thus, again there is no evidence of any dimensional changes in the first stage film which would have been indicative of development of material within the anodic film.

(*f*) *Extent of migration of molybdenum species: duplex films formed in molybdate electrolytes*

For the film containing the molybdenum tracer, shown in figure 6, the position of the tracer can be measured with respect to the metal/film and film/electrolyte interfaces. Thus, the location of the centre of the molybdenum-contaminated layer (the edges are relatively diffuse and do not allow precise definition) is 0.64 ± 0.01 with reference to the metal/film interface and 0.36 ± 0.01 with reference to the film/electrolyte interface, expressed in both cases as a fraction of total film thickness. Furthermore, the measured location can be compared with that predicted from the anodizing voltages and the relative migration rates of molybdenum species (0.20 ± 0.02), aluminium species (0.40 ± 0.02) and oxygen species (0.60 ± 0.02), derived from measurements with respect to implanted xenon marker layers for specimens anodized only once (Skeldon *et al.* 1985; P. Skeldon, G. E. Thompson & G. C. Wood, unpublished work). The predicted values are 0.62 ± 0.02 and 0.38 ± 0.01, indicating good agreement with the measured values.

Similar measurement and prediction were made for the location of the molybdenum-contaminated layer revealed in figure 8, where the film was formed exclusively in 0.1 M molybdate electrolyte avoiding any possible interference in the

Downloaded from rsta.royalsocietypublishing.org

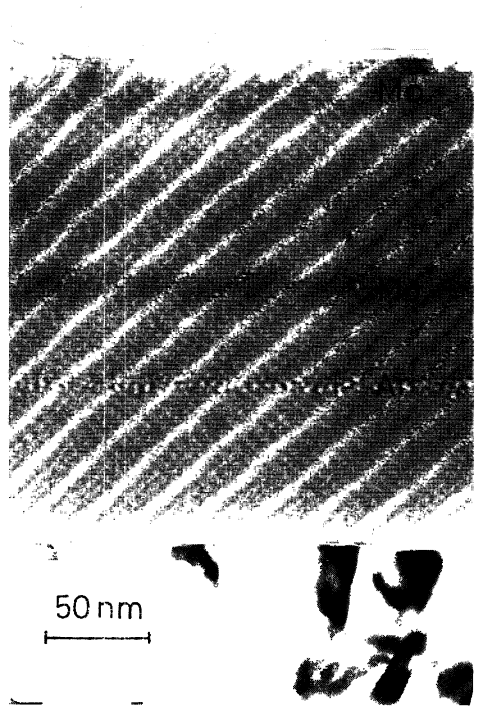

Figure 8. Transmission electron micrograph of an ultramicrotomed section of the anodic film attached to the ion plated aluminium substrate. The first anodizing stage involved film formation to 75 V at 50 A m^{-2} in 0.1 M sodium molybdate electrolyte at 293 K; the second stage involved re-anodizing to 202 V under the same conditions. The molybdenum species containing regions (Mo) and the argon bubbles (Ar) are indicated.

growth from incorporated borate. The measured values of the location of the centre of the tracer layer, referenced to the metal/film and film/electrolyte interfaces, expressed as fractions of the total film thickness, are 0.52 ± 0.01 and 0.48 ± 0.01, which compare well with the predicted values of 0.54 ± 0.01 and 0.46 ± 0.01.

The data indicate that the relative migration rate for molybdenum species, determined previously for a single anodizing stage, accounts for its movement in the films employed here and there are no significant changes in mobility within the region of film in which it has migrated, i.e. no major field non-uniformity. The magnitude of errors associated with the data indicated that the mobility is constant to within 10%.

(*g*) *Film composition: duplex films formed in tungstate electrolytes*

Ideally, for consistency with data given previously, compositional analysis of duplex films formed in molybdate electrolyte is preferred. However, more extensive contaminated layers develop as a result of anodizing in tungstate electrolyte, with greater tungsten species incorporation than molybdenum species (Skeldon *et al.* 1989). Thus, for improved precision of analysis, films containing an outwardly mobile tungsten species tracer were adopted.

The composition of films formed by the two stage anodizing procedure was

Downloaded from rsta.royalsocietypublishing.org

determined by RBS. A film formed exclusively in 0.1 M tungstate electrolyte (first stage 100 V, total voltage 190 V) was found to have an average composition $Al_2O_{3.0\pm0.1}$ $W_{0.018\pm0.001}$, similar to the composition of films formed under the usual anodizing conditions (Skeldon *et al.* 1985). Furthermore, the ratio of the tungsten yields from the first stage and second stage contaminated layers was 1.19 ± 0.02, compared with the predicted value from the anodizing voltages of 1.11 ± 0.04, assuming a constant rate of tungsten species incorporation with anodizing voltage (Skeldon *et al.* 1989). Generally good agreement exists although the value is slightly higher than predicted, perhaps attributable to slight differences in anodizing conditions during the two stages.

Furthermore, the RBS data gave no evidence of any redistribution of species from the contaminated layers, i.e. of transport to other film regions at concentration levels insufficient for direct observation in the transmission electron microscope. Thus, the substrate reversal procedure and subsequent re-anodizing do not influence the rate of incorporation of electrolyte-derived species to develop the tracer layers.

(*h*) *Duplex films formed in chromate electrolytes*

Anodizing in chromate electrolytes results in a tracer containing outwardly mobile chromium species, behaviour that is broadly similar to anodizing in molybdate and tungstate electrolytes; further examination of this behaviour is conducted here. From previous observations of films formed to 125 V during a single anodizing stage in chromate electrolyte, a relatively narrow band containing chromium species, observable by atomic number contrast, lies at a relative depth of 0.15 of the total film thickness, measured from the film/electrolyte interface to the mid-point of the band. Furthermore, the film regions above the band, extending to the film/electrolyte interface, also contain chromium species but at a concentration insufficient for atomic number contrast in the TEM (P. Skeldon, K. Shimizu, G. E. Thompson & G. C. Wood, unpublished work).

In this case a duplex film was formed exclusively in 0.1 M chromate (80 V first stage; 125 V total) with the final voltage corresponding to the dielectric breakdown voltage. The ultramicrotomed section of figure 9 reveals two bands passing approximately parallel to the metal/film and film/electrolyte interfaces; the light band located nearer to the metal/film interface represents argon bubbles and the more distant dark band is where the chromium species contaminant from the first stage of anodizing resides.

The region of film below the argon etch band is of relative thickness 0.23 ± 0.02 compared with a value of 0.22 ± 0.01, predicted from the usual nm V^{-1} ratio and the voltages of the individual anodizing stages. Thus, duplex film growth proceeds in the expected manner. The location of the chromium species tracer is 0.16 ± 0.01 measured from the argon band, which can be compared with a predicted value of 0.10 ± 0.01 for an immobile contaminated layer. Thus, the data show that chromium species migrate outwards at a rate of *ca.* 40% of the migration rate of aluminium species.

The previous data indicate that duplex film development in chromate electrolyte proceeds as expected from consideration of the relative migration rates of species contributing to film growth and, at face value, is little different from that proceeding in tungstate and molybdate electrolytes. However, unusual behaviour is evident for duplex anodizing in chromate electrolytes. Thus, the chromium species tracer is associated with fine cracks or voidage which developed during the second anodizing

Downloaded from rsta.royalsocietypublishing.org

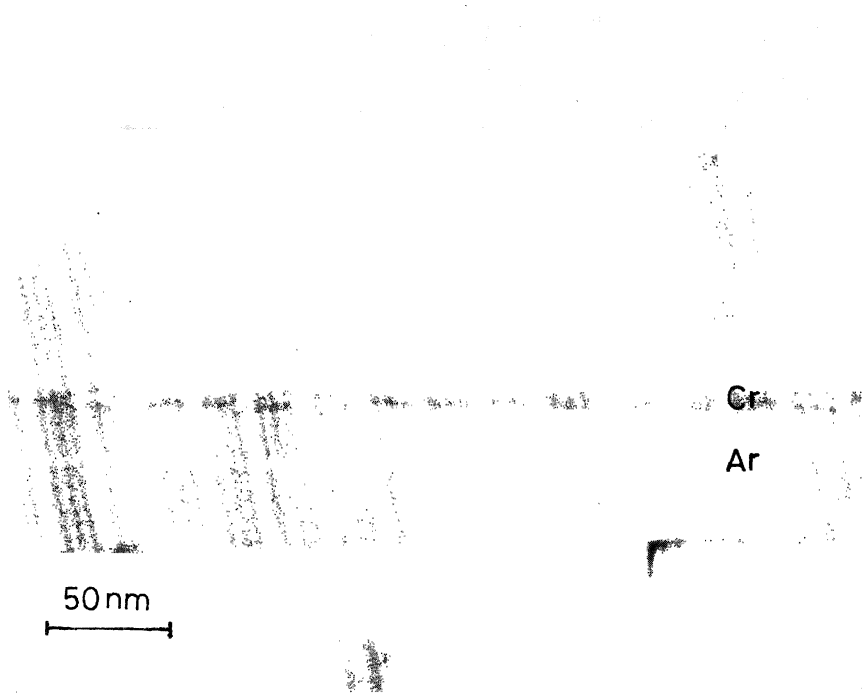

Figure 9. Transmission electron micrograph of an ultramicrotomed section of the anodic film attached to the ion plated aluminium substrate. The first anodizing stage involved film formation to 80 V at 50 A m^{-2} in 0.1 M sodium chromate electrolyte at 293 K; the second stage involved re-anodizing to 125 V under the same conditions. The chromium species containing region (Cr) and the argon bubbles (Ar) are indicated.

stage, as similar features have never been observed in sections of films resulting from a single anodizing stage. Additionally, no chromium species contaminated layer is evident in the outer film regions as a consequence of anodizing in the second stage. The lack of observation of the contaminated layer does not imply no incorporation of chromium species; rather such species have not concentrated sufficiently in appropriate film regions to develop the discrete band. This is possibly due to the relatively low voltage increment (45 V) during the second stage, but is unlike the behaviour associated with molybdenum and tungsten species (Skeldon *et al.* 1989). The ability of chromium species to develop the band may indicate their presence in the film as different species of varying outward mobilities, or may suggest differing coordination with oxygen in the alumina film structure. Concerning the inner band, the development of voidage during re-anodizing may then be associated with the presence of different chromium species within the film and their transformations under the field, which allow concentration within the tracer layer during further film thickening. Voids have been observed previously in alumina films, specifically during anodizing of hydrothermally treated aluminium when transformation of hydrated alumina to γ alumina causes shrinkage and fine porosity (Shimizu & Kobayashi 1985). In the present case it is difficult to envisage a similar conversion although it is possible that the presence of sufficient chromium species may encourage crystalline (γ or γ') alumina formation under the field. Certainly ruby-like films may be

Downloaded from rsta.royalsocietypublishing.org

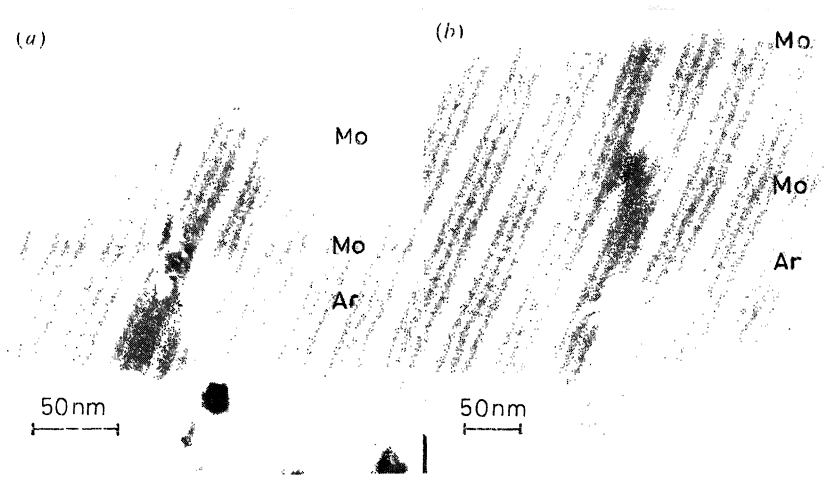

Figure 10. Transmission electron micrographs of the anodic film attached to the ion plated aluminium substrate. (*a*) Flaw region present above the argon etch band. (*b*) Flaw region which has influenced film growth locally during the second anodizing stage. The molybdenum species containing region (Mo) and the argon bubbles (Ar) are indicated.

developed from porous anodic films contaminated with chromate species, after a second anodizing stage at temperatures above ambient in a melt (Mita & Yamada 1980).

(*i*) *Film growth and the role of flaws*

A further application of mobile tracer layers is in the observation of local film growth in the vicinity of flaws; examples are given in figure 10 for the film formed exclusively in molybdate electrolyte. Figure 10*a* shows a flaw lying above the argon etch band, i.e. originally within the first stage region of the film. Near to the flaw, the argon etch band, the contaminated layers and the metal/film and film/electrolyte interfaces each bend outwards, forming small ridges above one another as if unbalanced alumina film growth had pushed outwards the wedge of film containing the flaw and deformed all boundaries/interfaces in the wedge, even though the general pattern of film growth within the wedge is relatively unaffected. A further explanation is that the possible impurity material contribution to the flaw, i.e. iron-rich segregates, has oxidized to produce a relatively voluminous material within the anodic alumina. A crack runs from the flaw to the film/electrolyte protuberance although it is not possible to say whether it opened during sectioning. Outside of the flaw and its zone of influence, film growth over the macroscopic alumina surface follows the usual behaviour. Figure 10*b* shows a second flaw which appears to have resided originally at the film/electrolyte interface after the first stage of anodizing (possibly contamination or generated in ion-plating). Within the zone of influence of the flaw, the film has been considerably altered compared with adjacent regions. At the flaw site the argon etch band has been obliterated; the metal/film interface is recessed through film encroachment around the flaw. The contaminated layer has been pushed significantly outwards towards the film/electrolyte interface, although the bulge on the latter is less noticable. The appearance suggests that the film has cracked above the flaw during the second growth stage (possibly the crack in figure

Downloaded from rsta.royalsocietypublishing.org

10*a* is relevant here) and subsequently healed by rapid local film formation at high current density.

Overall, the population density of flaws of the type revealed in figure 10 is low for the superpure aluminium used here; consequently they do not have a significant influence on the general film growth over the aluminium substrate. This situation could be altered with use of alloy substrates, thereby increasing flaw population densities.

4. Conclusions

1. This study has demonstrated that contaminated layers can be successfully introduced into anodic films on aluminium and, as tracers, they can be used to study film growth processes.

2. Growth of anodic films is shown to occur at the metal/film and film/electrolyte interfaces with no evidence of film formation within the alumina bulk.

3. The movement of the molybdenum-contaminated tracer layers with respect to the metal/film and film/electrolyte interfaces can be readily predicted from previously determined relative migration rates for molybdenum species, aluminium species and oxygen species. Thus, no variation in mobility of molybdenum species tracer layers is evident within the film, indicating the apparent uniformity of field strength across the film section and absence of significant space charge effects.

4. Other examples of the utility of the technique are provided by observations of the unusual behaviour in a chromium-contaminated layer, thought to be associated with crystalline alumina formation, and in studying local events around flaws, where the effects of local current concentration are revealed.

We thank the Science and Engineering Research Council for the award of a Research Assistantship to P.S. and the Royal Society for a Guest Visiting Fellowship taken up by K.S.

Appendix

This study has made effective use of contaminated film regions, displaced from and/or developed at their usual locations, to determine important features associated with the anodic alumina film growth process. Thus, the location of the mid-position of the outwardly mobile molybdenum-species contaminated tracer layer with respect to the relatively uniform metal/film and film/electrolyte interface can be determined readily and with appropriate precision. Comparison with predicted values, determined from the usual nm V^{-1} ratio for film growth and knowledge of the relative migration rates of the various cation and anion species, shows the validity of the overall approach.

In addition to use of the previous reference planes, the argon etch layer resident in the film sections may also be used. On the basis of earlier studies, such noble gas atomic markers are considered to be immobile and, at low concentrations, they do not influence anodic film growth to any significant extent (Pringle 1973, 1974). However, for this study, an immediate problem exists in that the marker layer is present as bubbles of finite width; furthermore, by creation of bubbles that are readily observed in film sections, some spreading of the marker layer is likely. Consequently, care must be taken in the identification of the correct reference position of the marker layer, i.e. to a position above or below the argon bubbles.

PHILOSOPHICAL TRANSACTIONS OF THE ROYAL SOCIETY A MATHEMATICAL, PHYSICAL & ENGINEERING SCIENCES

PHILOSOPHICAL TRANSACTIONS OF THE ROYAL SOCIETY A MATHEMATICAL, PHYSICAL & ENGINEERING SCIENCES

Downloaded from rsta.royalsocietypublishing.org

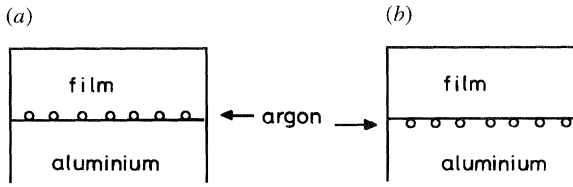

Figure 11. Schematic diagram showing possible locations of the argon after ion plating of aluminium on the surface of the anodic film formed on the electropolished aluminium substrate. (*a*) Argon located within the anodic film. (*b*) Argon located within the ion plated aluminium layer.

Table 1. *Average ratios of measured to predicted values of anion and molybdenum movements during the second stages of anodizing of duplex films*

reference position	anion	molybdenum
above Ar	0.94 ± 0.08	1.14 ± 0.12
below Ar	0.83 ± 0.06	1.38 ± 0.11

On the premise that the argon bubbles are initially located entirely within the first stage film (figure 11*a*), then new film formed by anion migration during the second stage is formed below this layer. Thus, measurements should be made to a reference plane just below the argon bubbles. Conversely, if the bubbles are located largely within the initial layers of ion plated aluminium, then the correct reference position is to just above the argon bubbles (figure 11*b*). In the light of this potential problem in determining the correct reference position, the films formed under the conditions of figures 6 and 8 have been used to determine the appropriate location. Table 1 gives the average ratios of measured to predicted values for the proportions of film formed by second stage anodizing and the accompanying molybdenum movements from reference to locations just above and just below the argon bubbles.

Reasonable agreement exists for measurements to a position just above the argon bubbles, suggesting that the argon is distributed between the first stage anodic film and the initial layers of ion plated aluminium adjacent to the film. Further confirmation is given by examination of a reference location to just below the marker layer which suggests a higher than normal rate of migration of molybdenum species and a significantly reduced (17%) extent of film growth at the metal/film interface by anion migration. Because the data presented earlier have shown no internal film growth and film thicknesses are proportional to the anodizing voltage, then any reduction in extent of film growth at the metal/film interface must be compensated by an increase in extent (26%) of film growth at the film/electrolyte interface by cation egress. This can be checked by measurement of the width of the tracer layer developed at the film/electrolyte interface after duplex anodizing in the molybdate electrolyte (figure 8). The relative thickness of 0.14 ± 0.01 agrees closely with predicted value of 0.13 ± 0.01, implying normal and anticipated anodizing behaviour. For the film grown in molybdate and then borate electrolytes (figure 6), partial film crystallization under the electron beam allows definition of the various contaminated film regions (figure 12) and assistance in resolving the preferred reference position. Thus, after partial crystallization, the outer film regions remain unchanged and hence, indicate the maximum possible film thicknesses contaminated with boron species. Close inspection of the outer film regions reveals a relatively light band above the molybdenum species layer; generally this change in contrast is evident prior to film crystallization and suggests that the narrow band is a region of

Downloaded from rsta.royalsocietypublishing.org

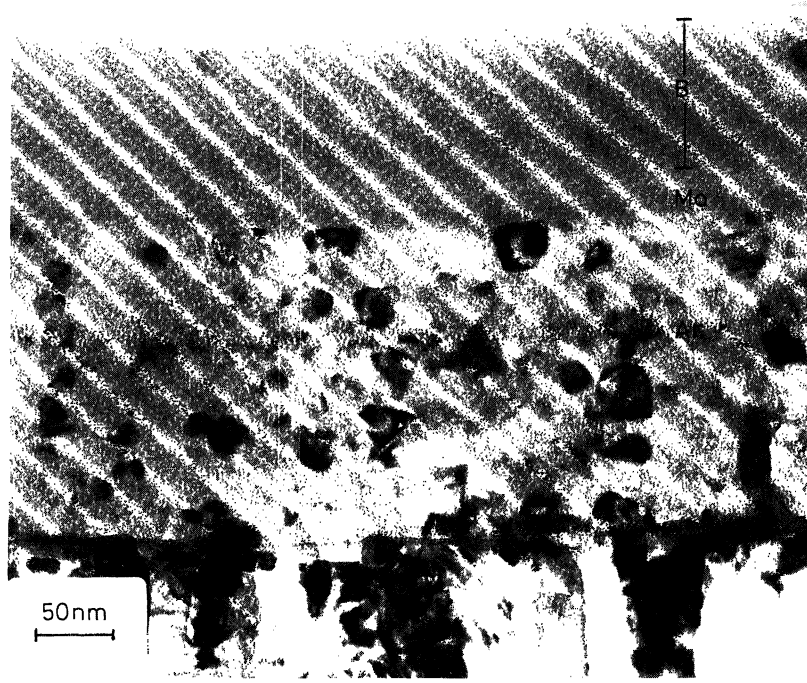

Figure 12. Transmission electron micrograph of an ultramicrotomed section of the anodic film attached to the ion-plated aluminium substrate. The first anodizing stage involved film formation to 75 V at 50 A m^{-2} in 0.1 M sodium molybdate solution at 293 K; the second stage involved re-anodizing to 295 V at 50 A m^{-2} in 0.01 M borate solution at 293 K. Electron beam induced crystallization reveals the relatively pure alumina film material. The boron (B) and molybdenum (Mo) species containing regions, and the argon bubbles are indicated.

uncontaminated alumina and its outer edge indicates the position of the film/electrolyte interface at the start of second stage anodizing. Using this reference position it is evident that boron species resides in the outer 0.31 ± 0.02 of the film compared with a predicted value of 0.30 ± 0.02. In light of this reasonable agreement it is concluded that film growth at the film/electrolyte interface proceeds as expected from behaviour discerned in single anodizing situations. Furthermore, it is concluded that the correct reference plane is a location just above the argon bubbles comprising the marker layer.

References

Amsel, G. & Samuel, D. 1962 The mechanisms of anodic oxidation. *J. Phys. Chem. Solids* **23**, 1707.

Brown, F. & Macintosh, W. D. 1973 The use of Rutherford backscattering to study the behaviour of ion implanted atoms during anodic oxidation of aluminium: Ar, Kr, Xe, K, Rb, Cs, Cl, Br and I. *J. electrochem. Soc.* **120**, 1096.

Davies, J. A., Domeij, B., Pringle, J. P. S. & Brown, F. 1965 The migration of metal and oxygen during anodic film formation. *J. electrochem. Soc.* **112**, 675.

Furneaux, R. C., Thompson, G. E. & Wood, G. C. 1978 The application of ultramicrotomy to the electronoptical study of surface films on aluminium. *Corros. Sci.* **18**, 853.

Hoar, T. & Mott, N. F. 1959 A mechanism for the formation of porous anodic oxide films on aluminium. *J. Phys. Chem. Solids* **9**, 97.

Downloaded from rsta.royalsocietypublishing.org

Mita, I. & Yamada, M. 1980 Ruby films formed on aluminium by anodic oxidation. In *Advanced metal finishing technology in Japan* (ed. N. Baba, T. Fukushima, K. Kuroda & T. Sato), p. 134. Tokyo: Fuji.

Pringle, J. P. S. 1973 Transport numbers of metal and oxygen during anodic oxidation of tantalum. *J. electrochem. Soc.* **120**, 398.

Pringle, J. P. S. 1974 Further observations on the marker behaviour of noble gases during anodic oxidation of tantalum. *J. electrochem. Soc.* **121**, 865.

Shimizu, K. & Kobayashi, K. 1985 Direct observations of voids and cracks in the barrier oxide layer of composite aluminium oxide films. *J. electrochem. Soc.* **132**, 1384.

Shimizu, K., Skeldon, P., Thompson, G. E. & Wood, G. C. 1982 Preparation of self-supporting anodic barrier films on aluminium. *Surf. Interface Anal.* **4**, 208.

Shimizu, K., Thompson, G. E. & Wood, G. C. 1981 Direct observation of the duplex nature of anodic barrier films on aluminium. *Thin Solid Films* **81**, 39.

Shimizu, K., Thompson, G. E., Wood, G. C. & Xu, Y. 1982*a* Direct observations of ion implanted Xe markers in anodic barrier films on aluminium. *Thin Solid Films* **88**, 255.

Shimizu, K., Thompson, G. E. & Wood, G. C. 1982*b* The duplex nature of anodic barrier films formed on aluminium in borate electrolytes. *Thin Solid Films* **85**, 53.

Skeldon, P., Shimizu, K., Thompson, G. E. & Wood, G. C. 1983 Barrier-type anodic films on aluminium in aqueous borate solutions: Part I and Part II. *Surf. Interface Anal.* **5**, 247 and 252.

Skeldon, P., Shimizu, K., Thompson, G. E. & Wood, G. C. 1985 Fundamental studies elucidating anodic barrier film growth on aluminium. *Thin Solid Films* **123**, 127.

Skeldon, P., Skeldon, M., Thompson, G. E. & Wood, G. C. 1989 Incorporation of tungsten and molybdenum species into anodic alumina films. *Phil. Mag.* **60**, 513.

Young, L. 1961 *Anodic oxide films*. London and New York: Academic Press.

Received 7 December 1992; accepted 5 May 1993

PHILOSOPHICAL TRANSACTIONS OF THE ROYAL SOCIETY A MATHEMATICAL, PHYSICAL & ENGINEERING SCIENCES

PHILOSOPHICAL TRANSACTIONS OF THE ROYAL SOCIETY A MATHEMATICAL, PHYSICAL & ENGINEERING SCIENCES

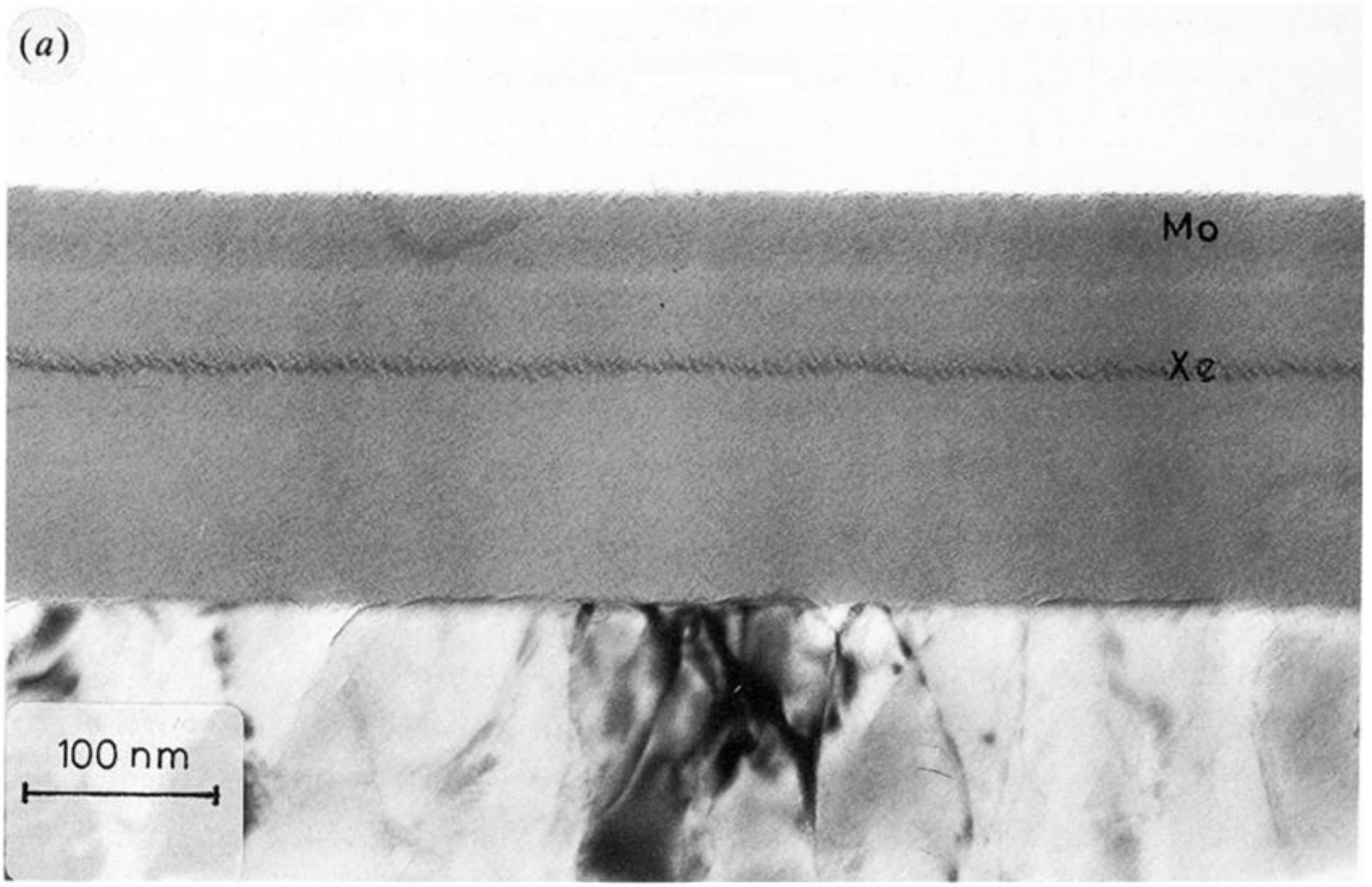

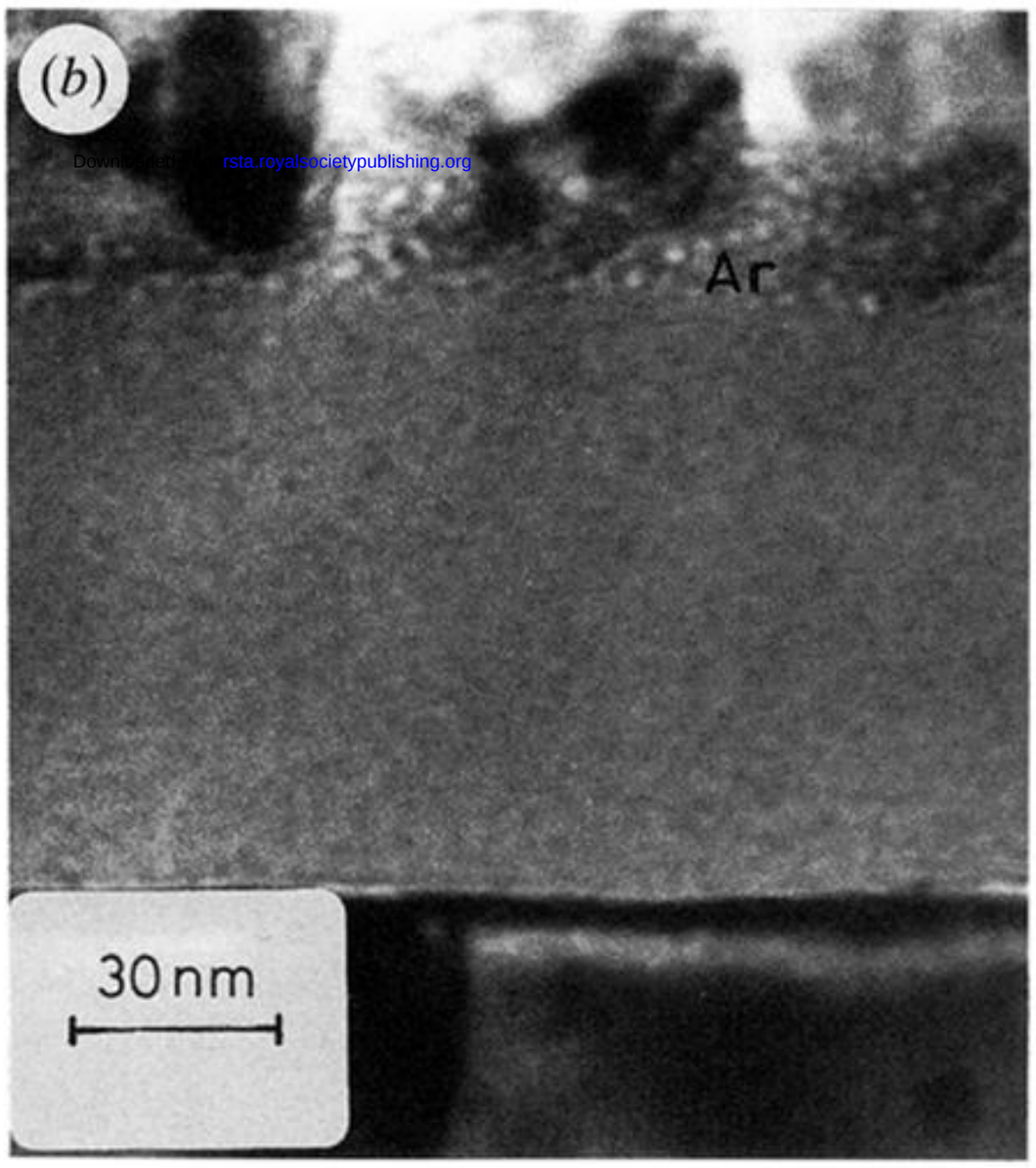

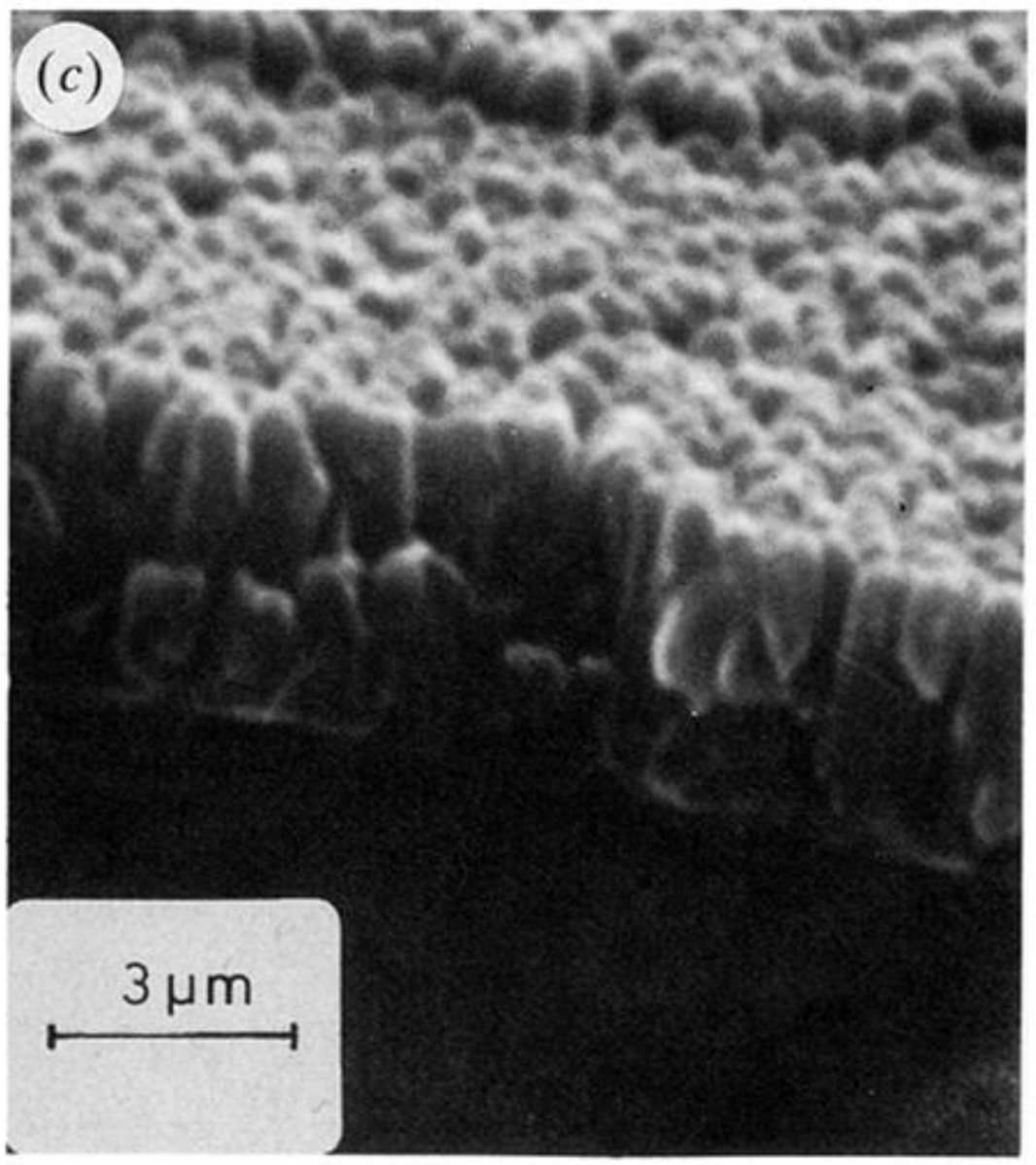

Downloaded from rsta.royalsocietypublishing.org

Figure 2. Electron micrographs of variously developed anodic alumina films on aluminium substrates. (*a*) Transmission electron micrograph of an ultramicrotomed section of the film formed on electropolished aluminium to 175 V at 50 A m^{-2} in 0.1 M sodium molybdate electrolyte at 293 K. (*b*) Transmission electron micrograph of the ultramicrotomed section of the original anodic film, formed to 75 V at 50 A m^{-2} in 0.1 M sodium molybdate electrolyte at 293 K, sandwiched between the ion plated aluminium and original electropolished aluminium substrate. (*c*) Scanning electron micrograph of the fracture section of the ion plated aluminium, showing the columnar grain appearance.

PHILOSOPHICAL TRANSACTIONS OF THE ROYAL SOCIETY A MATHEMATICAL, PHYSICAL & ENGINEERING SCIENCES

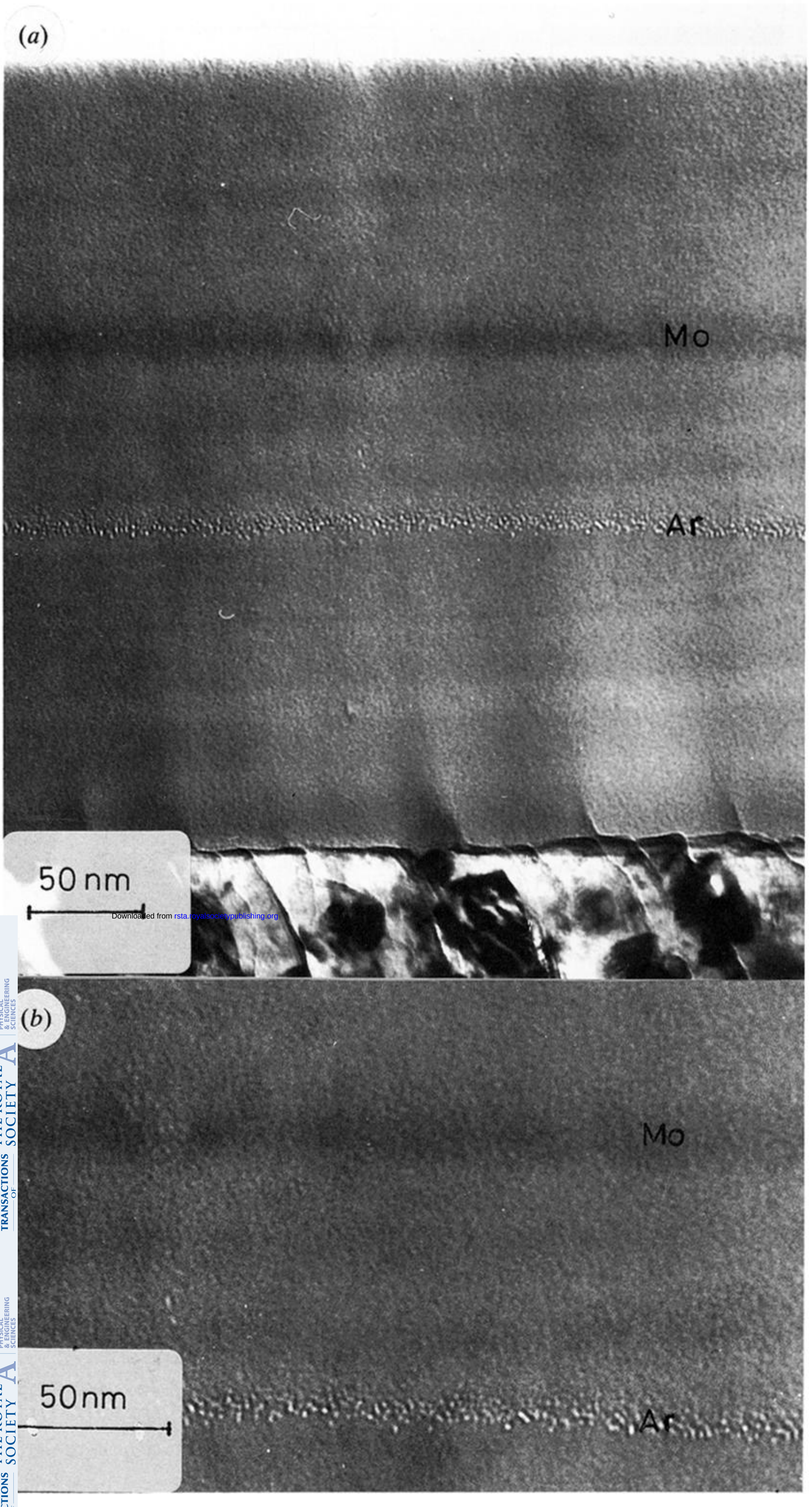

Downloaded from rsta.royalsocietypublishing.org

PHILOSOPHICAL TRANSACTIONS OF THE ROYAL SOCIETY A MATHEMATICAL, PHYSICAL & ENGINEERING SCIENCES

Figure 6. For description see opposite.

Downloaded from rsta.royalsocietypublishing.org

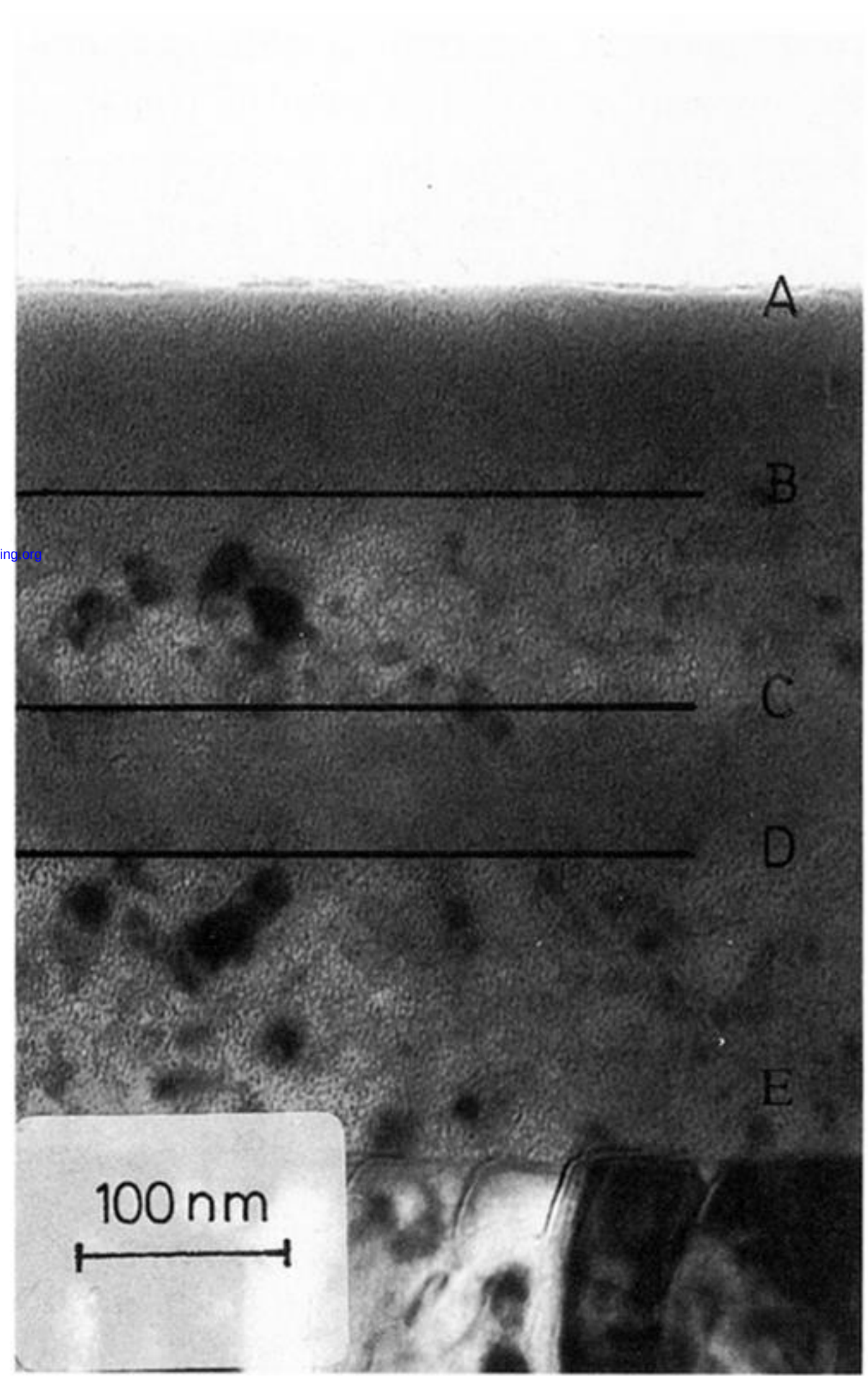

igure 7. Transmission electron micrograph of an ultramicrotomed section of the anodic film tached to the ion plated aluminium substrate. The first anodizing stage involved film formation 150 V at 50 A m^{-2} in 0.1 M ammonium pentaborate borate electrolyte at 293 K; the second stage volved re-anodizing to 355 V under the same conditions. Electron beam induced crystallization stinguishes the various film regions present: *AB* and *CD* are contaminated with boron species, hereas *BC* and *DE* are crystallized regions of relatively pure alumina.

PHILOSOPHICAL TRANSACTIONS OF THE ROYAL SOCIETY A MATHEMATICAL, PHYSICAL & ENGINEERING SCIENCES

Downloaded from rsta.royalsocietypublishing.org

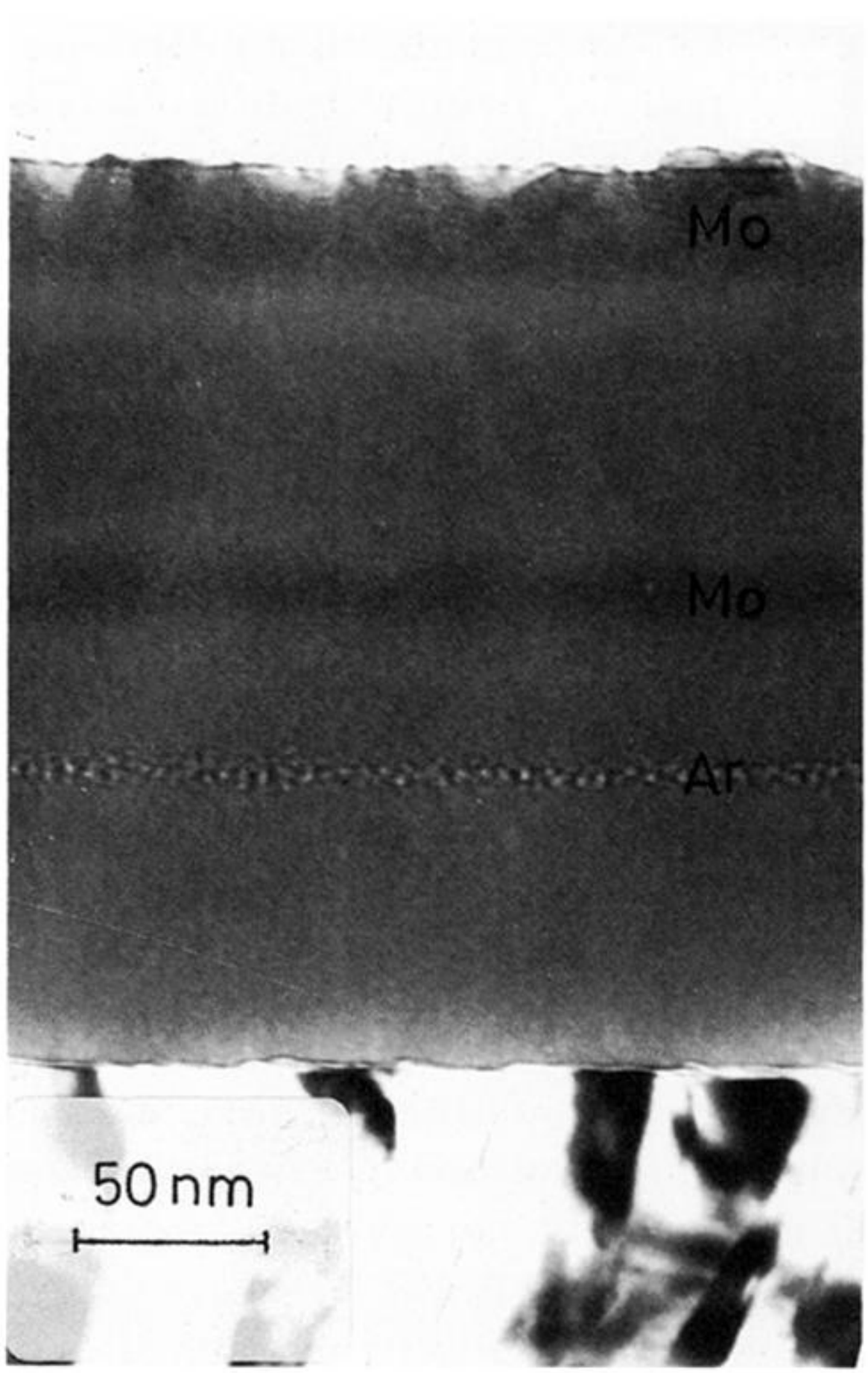

igure 8. Transmission electron micrograph of an ultramicrotomed section of the anodic film tached to the ion plated aluminium substrate. The first anodizing stage involved film formation 75 V at 50 A m^{-2} in 0.1 M sodium molybdate electrolyte at 293 K; the second stage involved re-odizing to 202 V under the same conditions. The molybdenum species containing regions (Mo) nd the argon bubbles (Ar) are indicated.

PHILOSOPHICAL TRANSACTIONS OF THE ROYAL SOCIETY A MATHEMATICAL, PHYSICAL & ENGINEERING SCIENCES

Downloaded from rsta.royalsocietypublishing.org

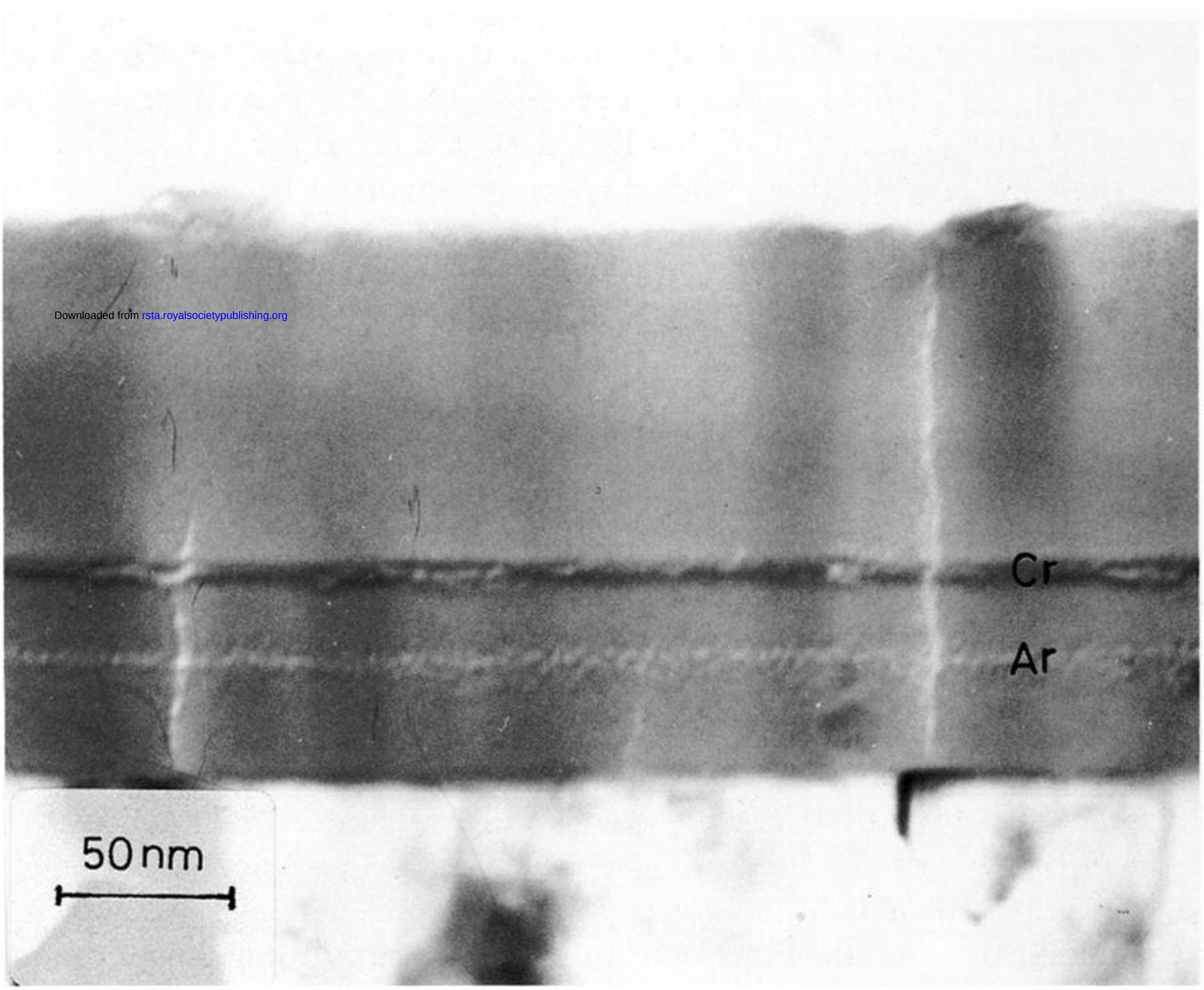

igure 9. Transmission electron micrograph of an ultramicrotomed section of the anodic film tached to the ion plated aluminium substrate. The first anodizing stage involved film formation 80 V at 50 A m^{-2} in 0.1 M sodium chromate electrolyte at 293 K; the second stage involved re-odizing to 125 V under the same conditions. The chromium species containing region (Cr) and e argon bubbles (Ar) are indicated.

PHILOSOPHICAL TRANSACTIONS OF THE ROYAL SOCIETY A MATHEMATICAL, PHYSICAL & ENGINEERING SCIENCES

PHILOSOPHICAL TRANSACTIONS OF THE ROYAL SOCIETY A MATHEMATICAL, PHYSICAL & ENGINEERING SCIENCES

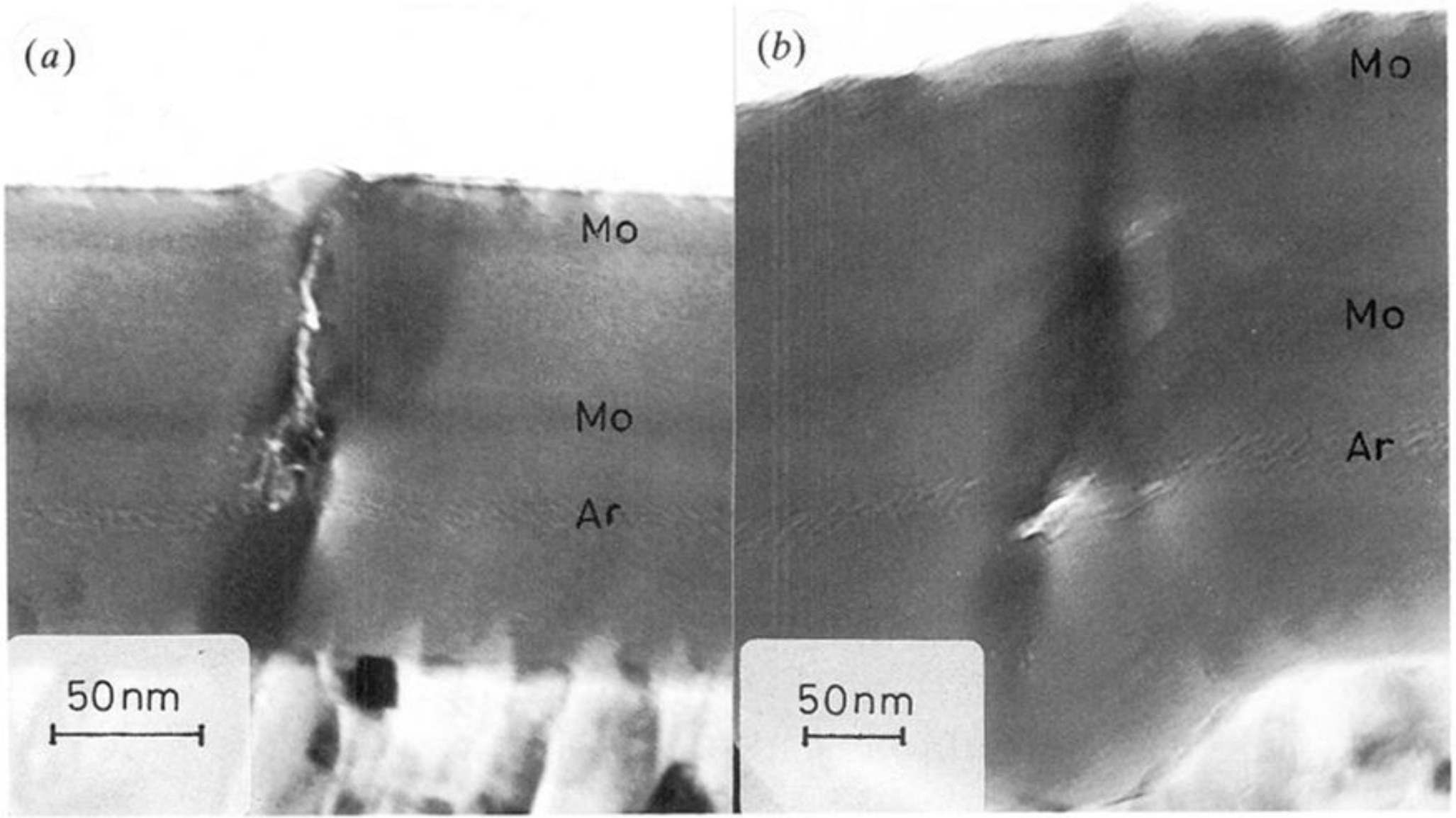

igure 10. Transmission electron micrographs of the anodic film attached to the ion plated luminium substrate. (*a*) Flaw region present above the argon etch band. (*b*) Flaw region which has nfluenced film growth locally during the second anodizing stage. The molybdenum species ontaining region (Mo) and the argon bubbles (Ar) are indicated.

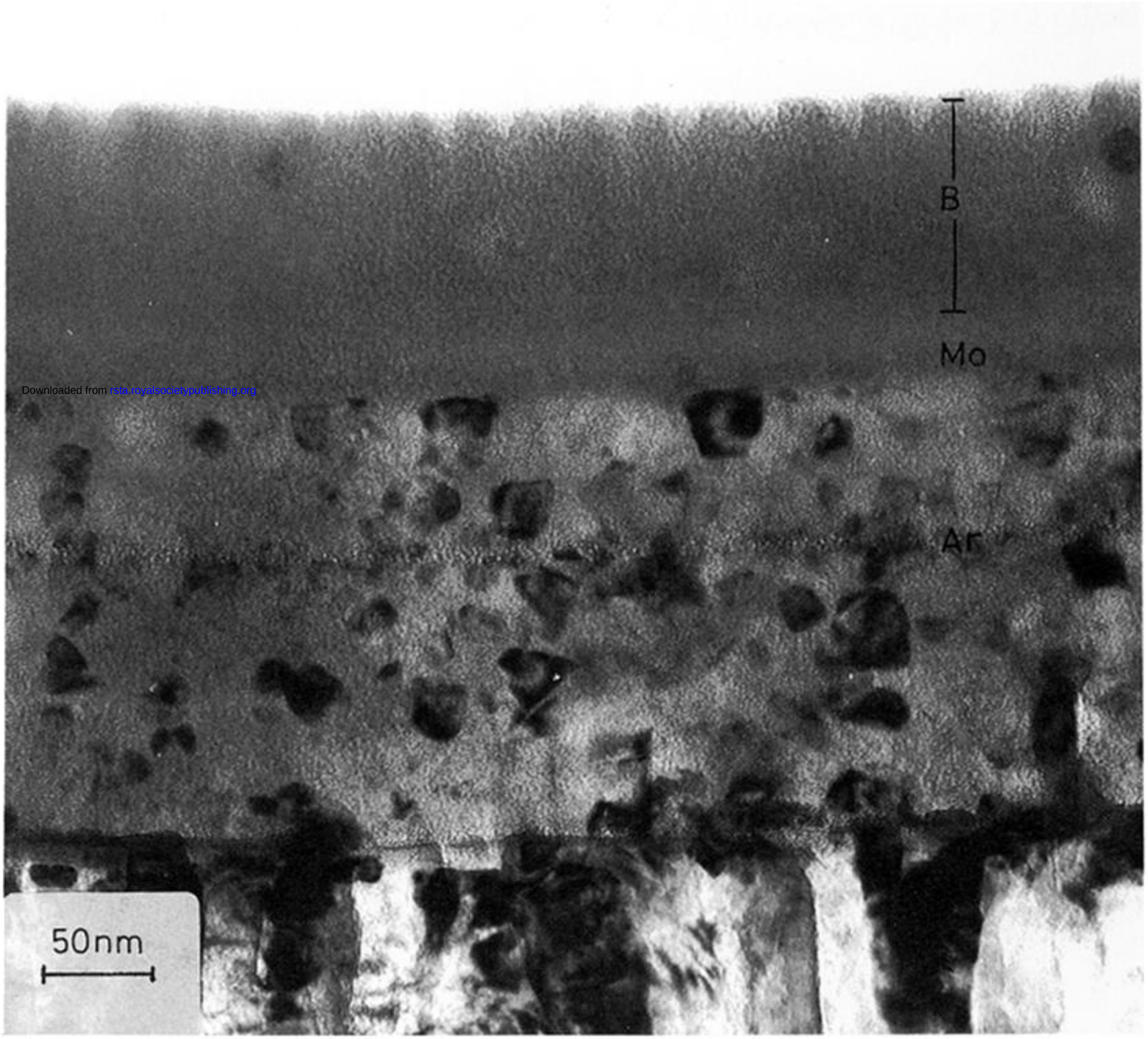

Downloaded from rsta.royalsocietypublishing.org

igure 12. Transmission electron micrograph of an ultramicrotomed section of the anodic film tached to the ion-plated aluminium substrate. The first anodizing stage involved film formation 75 V at 50 A m^{-2} in 0.1 M sodium molybdate solution at 293 K; the second stage involved re-odizing to 295 V at 50 A m^{-2} in 0.01 M borate solution at 293 K. Electron beam induced ystallization reveals the relatively pure alumina film material. The boron (B) and molybdenum Mo) species containing regions, and the argon bubbles are indicated.

PHILOSOPHICAL TRANSACTIONS OF THE ROYAL SOCIETY A MATHEMATICAL, PHYSICAL & ENGINEERING SCIENCES